

CHAPTER 1

Introduction

1.1. GENERAL INTRODUCTION

Probably the first reference of organic compounds bearing metallic nature dates back to the beginning of the last century. In 1910, McCoy and Moore prepared and isolated a tetramethyl ammonium amalgam by electrolysis, which showed certain physical properties associated to metals.¹ The authors concluded that “*it was possible to prepare composit metallic substances from non-metallic constituent elements*”.

In the 1950s, Akamatu *et al.* studied the electrical conductivity of polycyclic aromatics such as perylene **1**.² Even if these compounds were not conductors *per se*, the formation of complexes with halogens increased dramatically their conductivity ($\sim 1 \cdot 10^{-3} \text{ ohm}^{-1} \text{ cm}^{-1}$). It was suggested that the conductivity of these organic semiconductors was due to the intermolecular overlapping of π -orbitals present in these aromatic compounds.

In 1960, Kepler and co-workers prepared a series of organic semiconducting solids based on tetracyanoquinodimethane (TCNQ, **2**).³ The materials were metal salts of the radical cation of TCNQ $^{\cdot+}$ (with the following compositions: $M^+[\text{TCNQ}]^-$ and $M^+[\text{TCNQ}]^-[\text{TCNQ}]^0$) and showed the highest electrical conductivity of the time. Crystallographic studies showed that the face-to-face stacking of the TCNQ units was in keeping with the direction of the highest electrical conductivity (as anisotropy was observed). The electrical properties of the salts were justified by the formation of a degenerate system (similar to a metal) by the electrons of the radical anion.

A major breakthrough happened when in 1970, Wudl *et al.* prepared an organic stable radical cation based on the doping of tetrathiafulvalene (TTF, **3**) with chlorine.⁴ In 1973, Ferraris and co-workers prepared a highly conducting complex by mixing TTF and TCNQ.⁵ Conductivities as high as $6 \times 10^2 \text{ ohm}^{-1} \text{ cm}^{-1}$ at room temperature and $1.4 \times 10^4 \text{ ohm}^{-1} \text{ cm}^{-1}$ at 66 K were measured. The donor-acceptor complex was based on the formation of the radical cation of TTF and the radical anion of TCNQ (TTF $^{\cdot+}$ TCNQ $^{\cdot-}$) with a stoichiometry of 1:1. This complex was considered as the *first organic metal* and it gave rise to the preparation and

characterisation of a vast number of highly conducting charge transfer salts using these types of donors and acceptors.

In 1980, the first organic superconductor was synthesised by Bechgaard *et al.*⁶ The material was a salt based on a tetramethyltetraselenafulvalene (TMTSF, an all-selenium analogue of TTF), which acted as a donor, and an inorganic counteranion (PF_6^-) acting as an acceptor. The crystals were obtained by electrochemical oxidation of TMTSF in solution. TMTSF was used in the preparation of other superconducting salts with different anions (for example AsF_6^- , SbF_6^- , BF_4^- and NO_3^-), known as *Bechgaard salts*. Due to their pseudo-one-dimensional nature, the previous materials showed high anisotropy and electrical conductivity occurs mainly through the axis perpendicular to the stacking of TMTSF units.

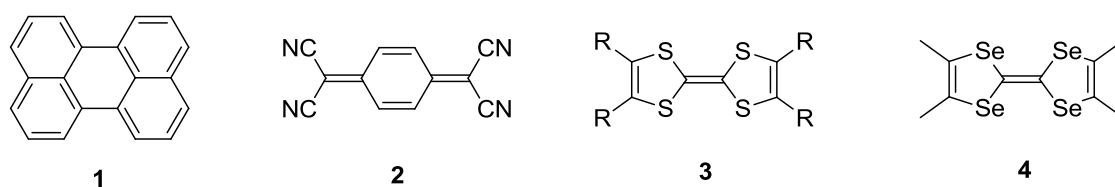


Figure 1.1. Chemical structure of perylene (1), TCNQ (2), TTF derivative (3) and TMTSF (4).

The problem was overcome by preparing salts based on bis-(ethylenedithio)-tetrathiafulvalene (BEDT-TTF, 5).⁷ The presence of four additional sulfur atoms (compared to TTF) enhances the non-covalent interactions, not only $\text{S}\cdots\text{S}$ but also $\text{C}\cdots\text{H}$, and usually leads to the formation of planes separated by the counter-anions. These compounds show a higher degree of order and are considered as quasi-two-dimensional superconducting organic compounds.

Another family of organic compounds has also shown electrical superconductivity. Although fullerene (C_{60} , 6) and most of its derivatives are insulators, they show superconductivity when they are doped with an alkali metal.⁸ Most of these superconductors have a general formula of M_xC_{60} where M can be a single alkali – metal or a combination of two of them to form binary alkali-metal compounds.

Because it has been shown that the critical temperature (T_c) is related to the size of the alkali-metal used in their preparation, cesium has been mainly used.⁹ However, these materials are chemically unstable and the sensitivity to ambient conditions is the main drawback of alkali-metal-doped fullerenes (A_xC_n).¹⁰

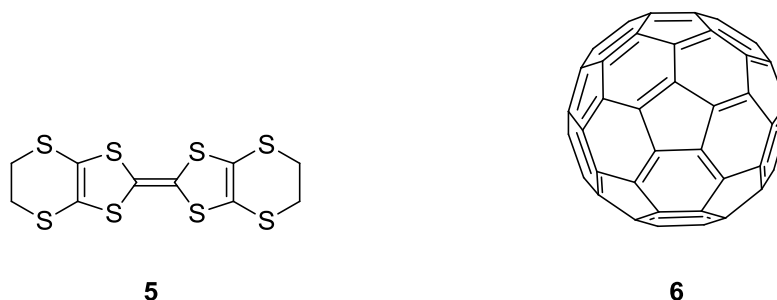


Figure 1.2. Chemical structure of BEDT-TTF (**5**) and C_{60} (**6**).

In parallel with the developments carried out for molecular organic materials as electrical semiconductors, polymers were also found to conduct electricity. Starting with the largely ignored initial studies carried out by Bolto and co-workers based on doped poly(pyrrole) in 1963,¹¹ and followed by the fabrication of switches with melanine by McGinness *et al.* in 1974,¹² the possibility of obtaining semiconducting polymers was shown.

In 1977, Shirakawa, Heeger and MacDiarmid reported the synthesis of a series of poly(acetylene)s and the preparation of highly conducting polymers by doping them with electron attracting species such as chlorine, bromine, iodine and AsF_5 .^{13,14} The doping process increased the electrical conductivity up to 10^{11} compared to the undoped polymers and conductivities of several hundred $\text{ohm}^{-1}\text{cm}^{-1}$ were measured at room temperature. The authors were awarded with the Nobel Prize in Chemistry in 2000 for “*the discovery and development of conductive polymers*”.

The key feature of conducting polymers is the presence of a highly conjugated system along the backbone of the polymer. The polymers bear a backbone of σ -bonds where the electrons are localized and π -bonds where electrons are not

localized so strongly. So that electrical conductivity can occur, the polymer has to be doped either by oxidation or reduction in order to generate partially occupied bands.

Following the growing interest in conducting polymers and to overcome the lack of stability of poly(acetylene)s under ambient conditions (they are sensitive to moisture and atmospheric oxygen), new conjugated polymers based on phenyl rings and on aromatic heterocycles have been widely synthesised. Undoubtedly, the most widely studied systems are poly(pyrrole), poly(aniline), poly(thiophene), poly(*p*-paraphenylenevinylene) and their derivatives.^{15,16}

1.2. BAND THEORY

The capacity of a solid to conduct electricity depends on the electronic structure of the material. Therefore, the electrical conductivity in solids can be explained by *band theory*. From the linear combination of N number of atomic orbitals, the formation of N number of molecular orbitals are obtained ($N/2$ bonding and $N/2$ anti-bonding). According to the principle of *Aufbau*, the electrons start filling first the bonding orbitals, as they are lower in energy, before they start occupying the higher orbitals in energy.^{17,18}

By following an analogous approach to the formation of molecular orbitals between the linear combination of atomic orbitals of the atoms present in a molecule, *solid orbitals* can be formed by the linear combination of the orbitals constituting the solid state (atoms, ions or molecules). Since in the solid-state the number of units (again atoms, ions or molecules) is very high and the combination of very similar orbitals in energy interact closely, the creation of energy bands is obtained. Since the bands are formed by a continuum of energy levels, discrete energies (like in atoms) do not exist and forbidden levels are not present. The highest energy band that is filled with electrons is called the *valence* band. On the other hand, the lowest vacant energy band is referred to as the *conduction* band.^{17,18,19}

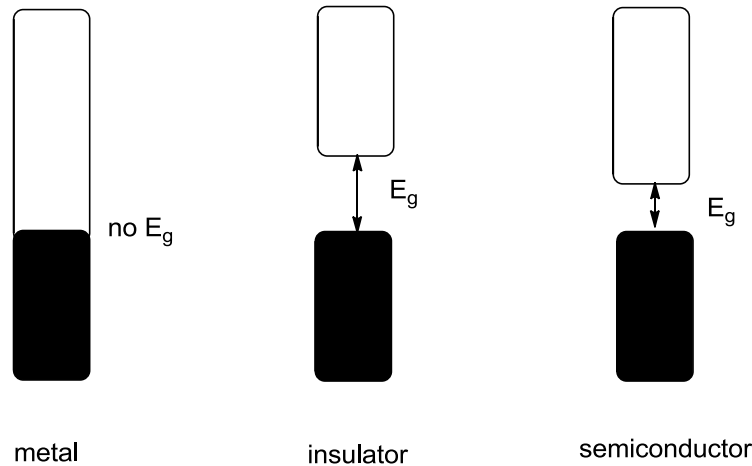


Figure 1.3. Schematic representation of the valence and conducting bands in solids.

In metals, the aforementioned energy bands overlap to form partially filled bands that favours electrical conductivity. The metals can be seen as a lattice of ions where the electrons move among them. There is no energy gap between bands and above 0 K electrons on the top energy levels of the valence band can gain thermal energy to occupy the conduction band. The conductivity in metals decreases when the temperature is raised as the thermal motion of atoms in the lattice scatter the electron mobility.^{17,18,19}

On the contrary, the difference between energy bands in some solids is so high that the electrons from the completely filled valence band cannot be promoted to the conduction band, which is empty. The difference in energy between the valence band and the conduction band is known as energy gap. Solids with E_g larger than *ca* 3.0 eV are considered as *insulators*. Insulators do not conduct electricity because the electrons are localised to form bonds, but because the bands are filled and there are not energy levels to which the electrons can be promoted by an electric field.¹⁹

Semiconductors can be considered as insulators with band gaps smaller than 3 eV ($E_g > 0$ eV), where electrons from the valence band can be promoted to the conducting band (a hole is left in the former band) for example by thermal excitation or photoexcitation. This type of semiconductor is referred to as an *intrinsic semiconductor*. At absolute zero, the valence band and the conduction band are

completely filled and empty, respectively, and therefore semiconductors do not show electrical conductivity at 0 K. Contrary to metals, the electrical conductivity increases exponentially with temperature as does the number of generated carriers (hole and electrons).^{17,18}

If the band gap of the solid is relatively wide, the material can be doped in order to decrease it. Doping of insulators is not enough to overcome the large band gap energy. The doping process of semiconductors consists of the incorporation of electron-donating or electron-accepting species into the solid which adds a new band of energy in between the valence and the conduction bands. These kind of materials are known as *extrinsic semiconductors*. By this decrease of band gap, the electrons can again be excited thermally to the conduction band.¹⁸

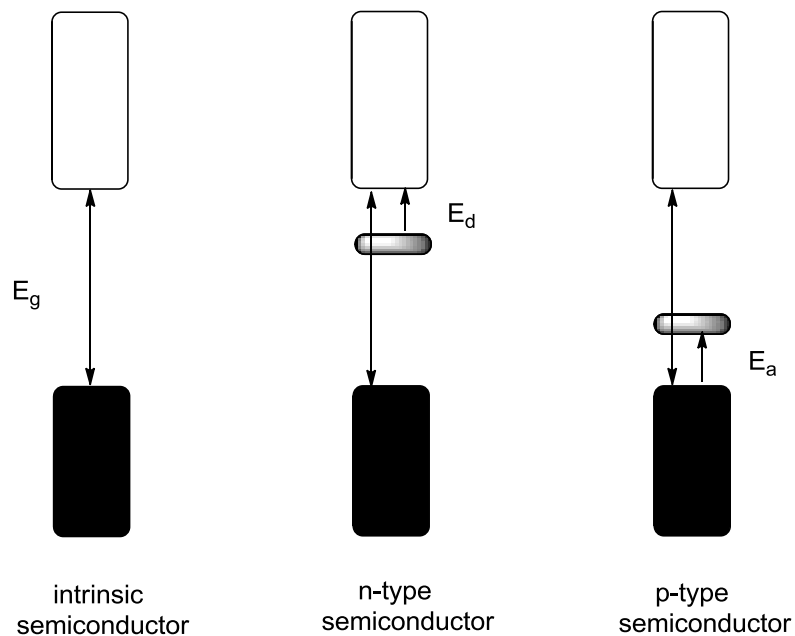


Figure 1.4. Schematic representation of the doping effect in semiconductors.

The classic examples to understand the doping process are the incorporation of elements of group III (boron, aluminum, gallium and indium), which act as electron acceptors, and group V (phosphorous, arsenic and antimony), which act as electron donors, into semiconductors of group IV (silicon and germanium). Doping with atoms from group III generates *p*-type semiconductors as they accept electrons from

the conduction band. On the other hand, doping with atoms of group V forms *n*-type semiconductors as they donate electrons into the conduction band of the solid.¹⁸

π -Conjugated systems consist of alternating single and double bonds. The backbone of these systems is formed by σ -bonds, whereas p-orbitals overlap with neighbouring orbitals to construct a conjugated system. The overlapping of these orbitals leads to the formation of HOMO and LUMO levels in the chains. By intermolecular interaction of the conjugated chain and in a similar fashion as mentioned above, the HOMO (π) and LUMO (π^*) levels form two energy bands. The HOMO orbitals form the π -band (or valence band which is filled) and the LUMO orbital the π^* -band (or conducting band). Depending on the nature of the constituents of the π -conjugated system, the value of band gap can vary, but it usually leads to semiconducting materials. By a similar analogy to inorganic compounds, the organic semiconductors can be *p*-doped or *n*-doped and electrical conductivity can be observed.

1.3. ENGINEERING OF THE ENERGY GAP IN π -CONJUGATED SYSTEMS

The control of the energy gap in organic semiconductors results of high importance in order to achieve the desired electronic properties in π -conjugated systems. The band gap of these materials has to be finely tuned depending on the application the organic material is to be used in (such as in organic photovoltaics, organic light emitting diodes or organic field-effect transistors). In general, low band gap materials are required to enhance the thermal excitation of the electrons to the conduction band and therefore increase the electrical conductivity. However, besides low band gaps, their relative positions *i.e.* the energy levels of the highest occupied molecular orbital (HOMO) and the lowest unoccupied molecular orbital (LUMO) are fundamental in many cases.

The band gap in these systems can be easily measured by UV-vis absorption spectroscopy or by cyclic voltammetry. In the former case, the band gap can be estimated from the onset of the lowest absorption band in energy. On the other hand, it can also be measured from the difference between the onset of the first oxidation wave and the onset of the first reduction process. Likewise, in both cases it can be determined in solution and in solid state.

The band gap of a linear π -conjugated system depends on five contributions *i*) Bond length alternation (BLA) contribution to the E_g ($E^{\delta r}$), *ii*) the mean deviation from planarity (E^θ), *iii*) the aromatic resonance energy of the cycle (E^{Res}), *iv*) the mesomeric or inductive electronic effects of the substituents (E^{Sub}) and *v*) the intermolecular effects (E^{int}).²⁰ Bearing this in mind, the E_g can be expressed as follows:

$$E_g = E^{\delta r} + E^\theta + E^{\text{Res}} + E^{\text{Sub}} + E^{\text{int}}$$

It has been seen that the molecular weight plays also a key role. However, the electron delocalisation is limited within the conjugation system and if the maximum effective conjugation length is surpassed (20-30 ring units for thiophene),²¹ the contribution to the opto-electronic properties is negligible (although physical properties can vary).

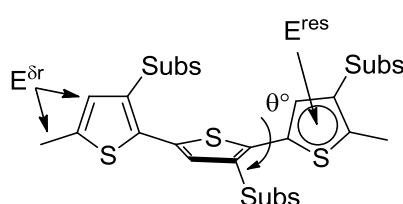


Figure 1.5. Schematic representation of the parameters that govern the band gap.

i) $E^{\delta r}$: In polyacetylene, if all the double bonds were completely delocalised, the polymer would become a metallic conductor as the band gap would decrease to 0. However, this situation is unstable and deformation towards alternation of single-

double bonds (bond length alternation) breaks the degeneration and leads to a finite E_g .²⁰

The degree of bond length alternation (BLA) is defined as the difference between the average length of single bonds and double bonds and it plays an important role in the analysis of the band gap.²² $E^{\delta r}$ represents the main contribution to the existence of a band gap.

One approach to decrease the BLA and therefore the band gap is by increasing the quinoid structure in polymers based on aromatic rings.²² In poly(thiophene), the quinoidal form is energetically unfavourable compared to the aromatic form which leads to an increase in the character of the single bond between rings. To increase the quinoidal form of the thiophene, Wudl and co-workers prepared poly(isothianaphthene) (PITN, **7**).²³ The higher resonance energy of the fused benzene ring, results in the dearomatisation of the thiophene rings. By increasing the quinoid form, the band gap of PITN decreased to 1.10 eV compared to poly(thiophene) (2.0 eV).²⁴

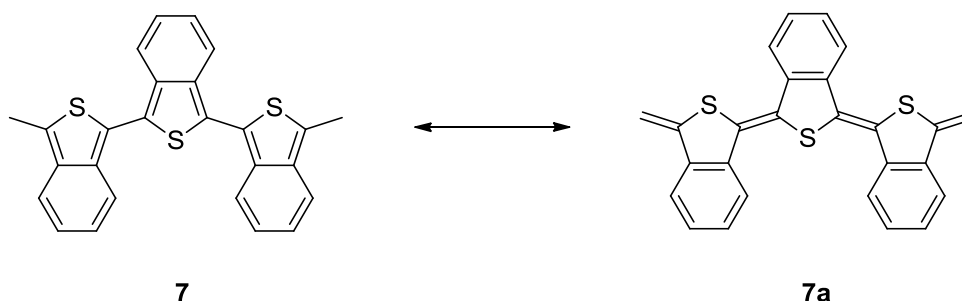


Figure 1.6. Aromatic and quinoidal conformations of PITN (**7**).

Most of the synthesised homopolymers in the literature have a band gap larger than 1.9 eV. In 1993, an innovative approach was developed by Havinga and co-workers to overcome this, that consisted of the alternation of donor (*e.g.* fused thiophenes, fluorene, carbazole) and acceptor (*ea.* benzothiadiazole and thienopyrazine) moieties along the backbone of the conjugated system.²⁵ An internal charge transfer process

from the donor to the acceptor occurs that increases the double bond character between units (BLA decreases) and therefore a lower band gap is achieved.

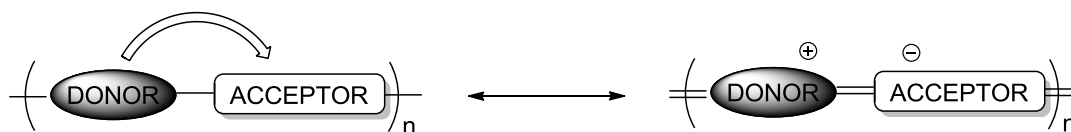


Figure 1.7. Donor-Acceptor approach.

ii) E^{θ} : The presence of single bonds between aromatic rings allows interanular rotations along the conjugated backbone. The effective conjugation can be disturbed by deviation from planarity due to a poor overlapping of the orbitals. The π -electrons become more localised and the E_g increases.

The substituents play a key role, as bulky groups can decrease the desired planarity of the backbone. On the other hand, smaller groups or by linking the aromatic units through covalent bonds (or non-covalent interactions) can enhance planarity.

iii) E^{Subs} : The most effective way to control the HOMO and LUMO levels, and therefore the E_g , of a compound is by incorporating substituents. Electron-donating groups (aliphatic chains, amines or alkoxy chains) push electron density into the system and increase the HOMO level. The incorporation of electron-withdrawing groups (cyano, trifluoromethyl or nitro) results in a decrease of the LUMO level as the reduction potential is lowered. The correct position of substitution of these groups is of high importance.

iv) E^{Res} : This contribution is related to the aromatic resonance energy of the aromatic rings. The aromatisation of the rings impedes the delocalisation of the π -electrons along the conjugated backbone. It has been seen that the incorporation of ethylene groups between aromatic rings diminishes the aromaticity of the system and therefore the E_g .²⁴

v) E^{Int} : Whereas the previous effects are related to the polymeric system, there is another contribution due to the spatial disposition that the conjugated system adopts

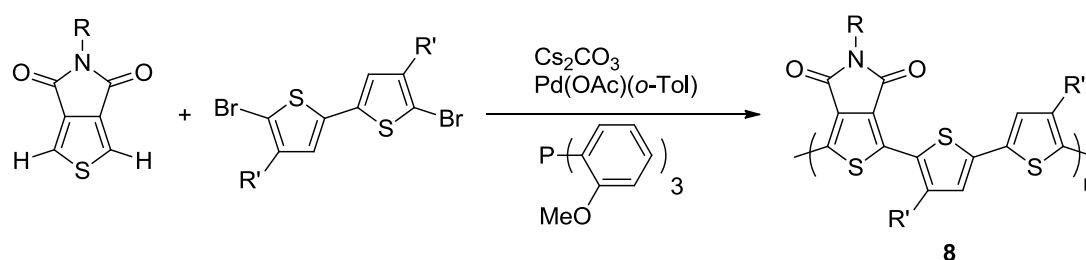
in the solid state (E^{Int}). The torsion angle of the polymeric units can be planarised by close π - π interactions, delocalizing the π -electrons and lowering the E_g .

1.4. SYNTHESIS OF π -CONJUGATED SYSTEMS

The synthetic methods used in the synthesis of conjugated systems have been developed greatly in order to obtain the best properties. One clear example is the synthesis of poly(3-hexyl-thiophene) (P3HT). Highly regio-regular P3HT is required in order to obtain better morphological properties leading to an increase in the device performance. Although a large number of polymerisation can achieve P3HT, only some of them obtain the regio-regular polymer.

The vast majority of conjugated systems contain aromatic units that are mainly obtained *via* metal-catalysed cross-coupling reactions. Undoubtedly, Stille and Suzuki coupling are the most widely used cross-coupling reactions. Other couplings such as Negishi, Kumada, Heck and Sonogashira are also used but to a lower extent.

Recently, direct heteroarylation has been successfully carried out to prepare a donor-acceptor conjugated polymer (see Scheme 1.1).^{26,27} Although the presence of catalytic amounts of metal is still required, the direct coupling of the units by C-H bond cleavage facilitates the synthesis of the precursors and can eliminate the synthesis of highly toxic intermediates used in Stille coupling.



Scheme 1.1. Synthesis of polymer **8** by direct heteroarylation.

1.4.1. Stille Coupling

Stille coupling is based on the cross coupling of an organohalide ($X = \text{I}, \text{Br}^-, \text{Cl}^-$) or pseudo-halide (such as triflate group) compound with an organotin derivative catalysed with palladium(0).²⁸ The reaction proceeds through a general mechanism (Figure 1.8.) based on (i) oxidative addition of the organohalide to Pd(0) (usually Pd(0)L_n), (ii) transmetallation of the resulting Pd(II) complex with the organotin derivative and (iii) reductive elimination to give the final product and recovery of the Pd(0).

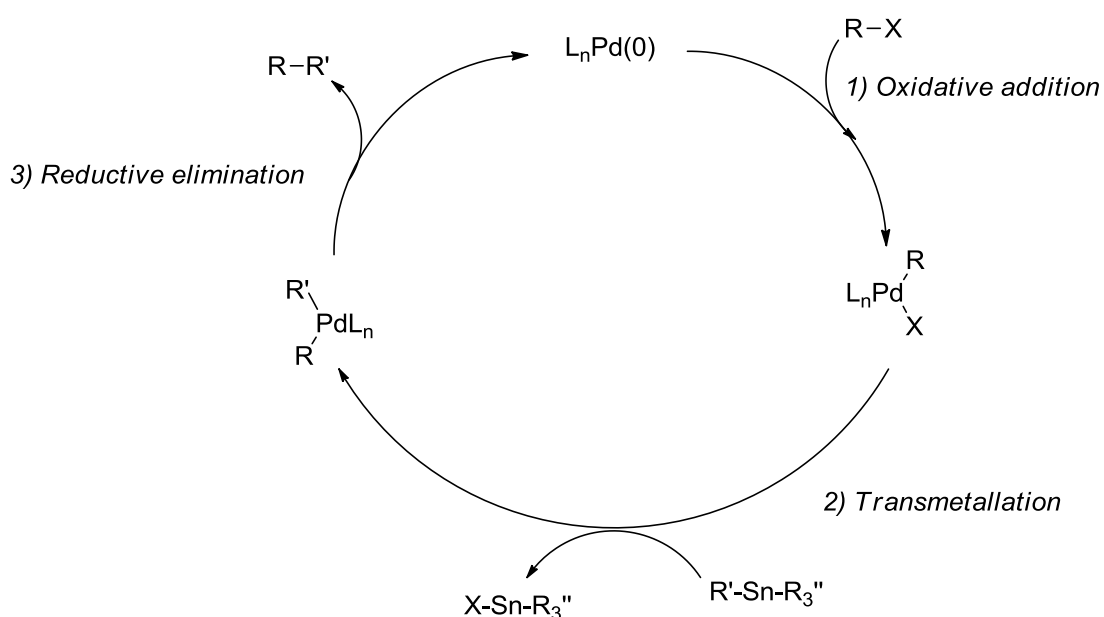


Figure 1.8. Mechanism of the Stille cross-coupling reaction.

The oxidative addition depends on the tendency of the halogen to act as a leaving group. Therefore, the greatest reactivities are observed with I and Br^- . The reaction with triflates also gives high yields but it usually requires the addition of LiCl . Generally, chlorinated aryls do not react in high yields due to the poor reactivity in this step. The transmetallation is usually the rate-determining step. The last step is rapid and irreversible and occurs when both coupling units adopt a *cis* conformation at the palladium centre.

Due to its high versatility (as most of the functional groups are tolerated), Stille coupling has been widely used in the preparation of conjugated systems.^{29,30} For the synthesis of conjugated polymers both derivatives have to be difunctionalised (X-Ar-X and R₃Sn-Ar'-SnR₃). In these cases, the organohalide is usually prepared on the electron-poor partner to facilitate the oxidative addition, whereas the organotin derivative is prepared on the electron-donor partner which enhances the transmetallation step (it can be seen as an electrophilic substitution).

Although, the Stille coupling reactions are typically carried out with Pd[PPh₃]₄, some systems might require the use of different catalysts, ligands or additives. Besides decreasing the reaction times, microwave-assisted Stille coupling polymerisations can increase considerably the molecular weights and lower the polydispersity of the polymers.³⁰ These improvements have been associated with the direct transfer of energy to the reactants. The main drawback of this reaction is the high toxicity of the tin derivatives such as Me₃SnCl that is commonly used after lithiation to obtain the organotin derivatives.

1.4.2. Suzuki Coupling

Suzuki-Miyaura coupling consists of the cross-coupling of an organohalide (X= I, Br⁻, Cl⁻) or pseudo-halide (such as triflate group) with organoboron derivatives.³¹ Boronic acids are the main organoboron derivatives, but boronic esters, organoboranes or trifluoroborates have also been widely used. The reaction mechanism is thought to be based on the same three steps (*i*) oxidative addition, (*ii*) transmetallation and (*iii*) reductive elimination (Figure 1.9.).

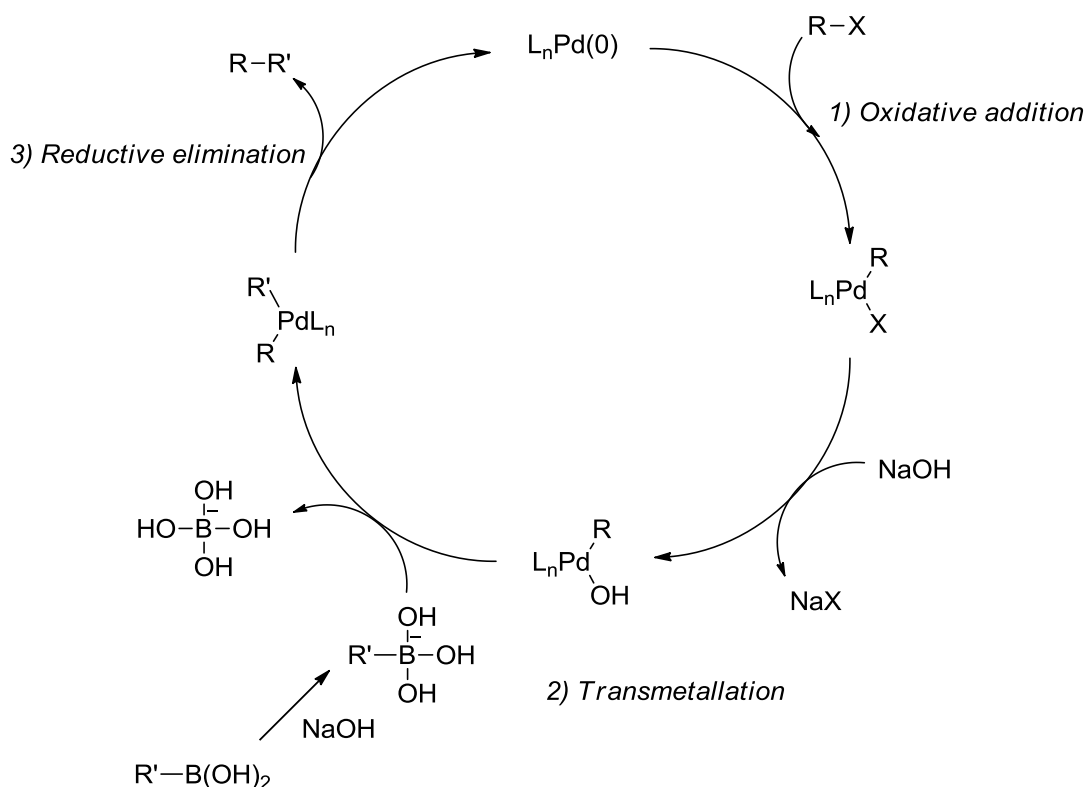


Figure 1.9. Mechanism of the Suzuki-Miyaura cross-coupling reaction.

The main difference of Suzuki coupling with other Pd-mediated cross-coupling reactions is the addition of an anionic base (for example OH^- , OAc^- , CO_3^{2-}) to activate the highly stable B-C bonds by forming a tetracoordinated boronate derivative. Equally, after the first step the halide is replaced by the anionic base in the catalytic centre. After the transmetalation step, the two coupling partners are linked by reductive elimination to obtain the final compound.

Suzuki coupling has been widely used in the preparation of conjugated systems. In order to obtain polymers, disubstituted organohalogenes and organoboron derivatives are required. $Pd[PPh_3]_4$ is usually used as catalyst, but due to its low reactivity in some cases other more reactive catalysts are required. Likewise, the presence of an adequate ligand can be crucial to achieve the desired product. For example bulky phosphine ligands are required for couplings with chlorinated derivatives.³² Typically solvents like tetrahydrofuran, toluene or dioxane are used. The need to solubilise the anionic base usually requires the addition of some water, which can

then lower the solubility of the conjugated polymer and lead to low molecular weights and high polydispersities.

1.4.3. Yamamoto coupling

The cross-coupling of two organohalide derivatives catalysed by a Ni(0) species is referred to as Yamamoto coupling. Dehalogenation polycondensation of disubstituted organohalides (thiophenes and benzene derivatives) yields π -conjugated polymers with high molecular weights.³³ Although the halogen plays an important role (reactivity I > Br > Cl), even dichlorinated derivatives give good yields. The yields are usually improved when Ni(cod)₂ (cod = cyclooctadiene) is used instead of Ni(PPh₃)₄.³⁴ Due to the relatively low reactivity of the Ni(0) species, conjugated polymers bearing functional groups such carbonyl and cyano can be prepared.

The mechanism of this polymerisation is different to the previous cross-coupling reactions, and was proposed by Yamamoto *et al.* in 1994.³⁵ The mechanism is depicted in Figure 1.10. The first step consists of an oxidative addition to the Ni(0) species. This species undergoes a disproportionation which is favoured by polar solvents (DMF is generally used for this reaction) and is followed by a reductive elimination to give a longer conjugated polymer bearing two bromine atoms at the end of the chains.

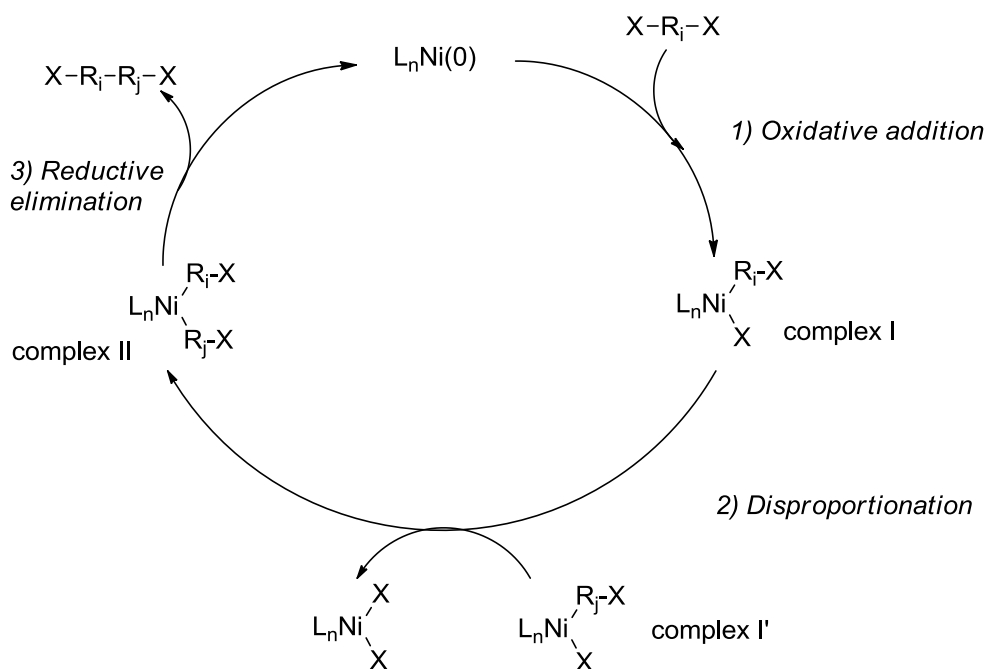


Figure 1.10. Mechanism of the Yamamoto reaction.

This method has been widely used in the preparation of poly(thiophene)s. The main advantage of this method is that branched polymers are not formed (only two peaks are observed in ^{13}C -NMR), as the polymerisation proceeds exclusively through the 2 and 5 carbons, giving rise to linear polymer.³⁶

Yamamoto coupling was also used to synthesise poly(3-alkyl-thiophene)s. Since the oxidative addition of a 5-X-thiophene to the Ni(0) complex is easier than the more sterically hindered 2-X-thiophene, the reaction does not give regio-regular poly(3-alkyl-thiophene)s but couplings of head-to-head with tail-to-tail units. The highly interesting regio-regular poly(3-alkyl-thiophene)s can be obtained by other coupling methods.³⁶

Although certain types of copolymers can be prepared *via* Yamamoto polymerisation, this reaction is not the best approach to obtain highly sought after alternating copolymers.

1.4.4. Sugimoto polymerisation

Sugimoto polymerisation is based on the oxidative polymerisation of aromatic heterocycles with ferric chloride.³⁷ The usually mild reaction conditions required to carry out the polymerisation (the monomer does not have to be derivatised, room temperature, dry chloroform) makes Sugimoto reaction an interesting method to obtain conjugated polymers. The reaction is usually bubbled with an inert gas to remove the HCl (g) formed when the reaction proceeds.

Although high molecular weights are usually obtained, the reproducibility of the reaction remains an issue.³⁸ One of the main advantages of this method is that the polymers can be easily obtained in bulk due to the low demanding conditions. In addition to this, by using excess of FeCl₃, the doped polymer can be obtained *in situ*. The doped polymer can be easily dedoped by using a reducing agent (*e.g.*, hydrazine).

This reaction has also been studied in the synthesis of regio-regular poly(3-alkyl-thiophene)s and it has been shown that the regio-selectivity can be to be up to 94 % (head-to-tail) when a bulky substituent is attached to the 3 position.³⁹

Several reaction mechanisms have been proposed for Sugimoto polymerisation. Radical polymerisation was first proposed by Niemi *et al.*⁴⁰ The ferric cation is reduced to the ferrous cation by thiophene. The oxidised radical-cation species dimerises and subsequent reaction propagates to form the polymer. The second mechanism considers that the propagation proceeds *via* a carbocation.³⁹ In this case, although the initiation species is a thiophene radical cation, the dicationic species formed in oligomeric chains act as an electrophile and undergo electrophilic aromatic substitution. Due to the high level of regio-regularity that is obtained, this mechanism might be more accurate as the radical propagation should give rise to lower regio-regularity. In both cases the initial step is believed to be the formation of the radical cation of thiophene.

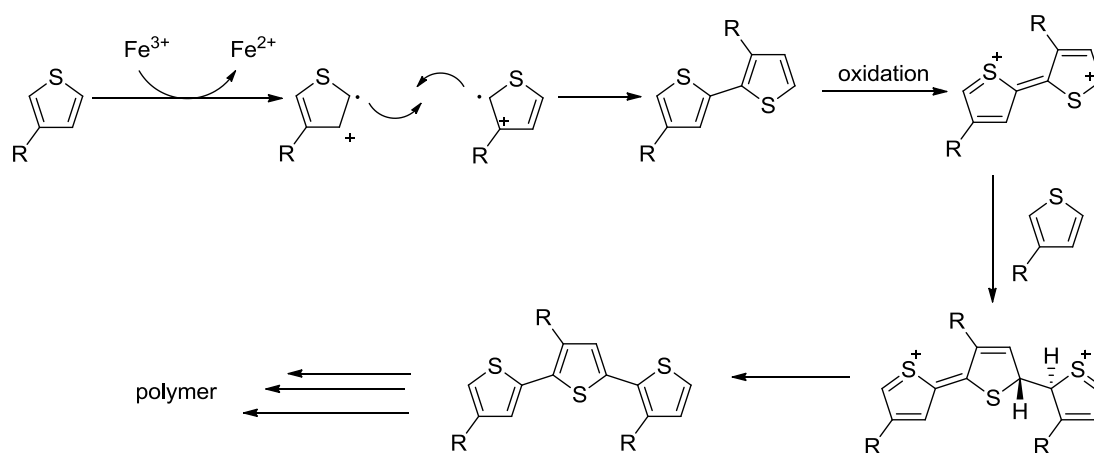


Figure 1.11. Mechanism of the Sugimoto oxidative polymerisation reaction.

1.4.5. Electropolymerisation

Electropolymerisation is a technique that allows the formation of conducting polymers on a working electrode. The polymers are deposited on an electrode (usually anode) by repetitive oxidation of the monomeric unit in solution in the presence of a supporting electrolyte. Although the polymer cannot be prepared in bulk, in comparison with other chemical oxidative polymerisations, electropolymerisation gives cleaner polymers with an easy control of the film thickness.

The three main ways used for electropolymerisation are potentiostatic, galvanostatic or potentiodynamic techniques. In potentiostatic electropolymerisations, a constant potential is applied to the solution, whereas in the galvanostatic technique the current is maintained constant. The main potentiodynamic technique is cyclic voltammetry, where the potential is sequentially scanned between two fixed potential values. Even though, the polymerisation can start at the voltage of the onset of the ionisation potential peak (it is usually the peak at lower voltage), the higher potential is usually fixed several hundreds of millivolts higher than the ionisation potential. This method allows the polymer growth to be followed as the polymeric chains show a new developing peak at lower voltage, as a result of the increasing conjugation.^{41,42}

Aromatic heterocycles have been mainly electropolymerised (*e.g.*, thiophene, pyrroles and their derivatives). The mechanism of the electropolymerisation is still controversial. It is accepted that the first step consists of the oxidation of the monomer to form the radical cation ($M^{\cdot+}$). The electron transfer reaction is generally faster than the diffusion of the radical cation in solution. Therefore, a high concentration of $M^{\cdot+}$ is located around the electrode and $M^{\cdot+}$ dimerises. The neutral dimer is obtained after loss of two protons and rearomatisation. The dimer, which due to extended conjugation is more easily oxidised, forms the radical cation and reacts with $M^{\cdot+}$ to form a trimer species. Rearomatisation and subsequent oxidations lead to the formation of the polymer which precipitates on the working electrode. A scheme of the mechanism is shown in Figure 1.12.

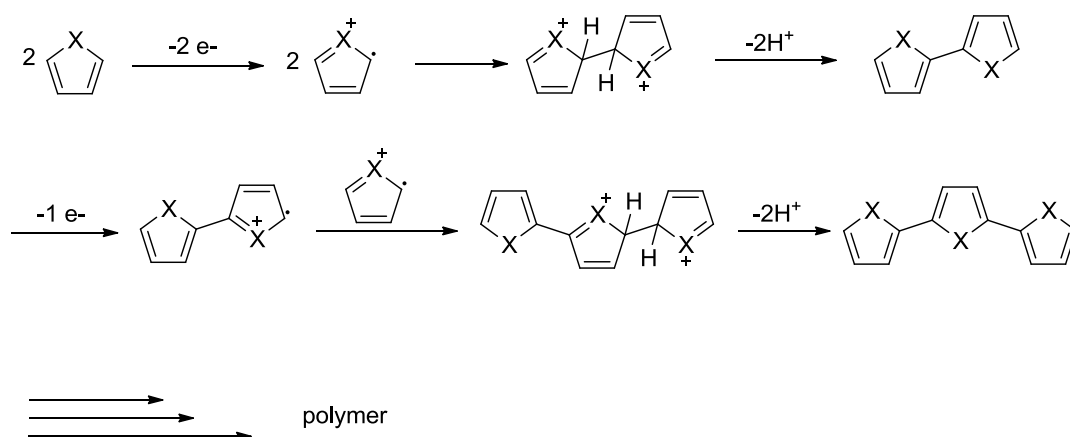


Figure 1.12. Mechanism of the electropolymerisation of five-member rings.

Since the growing polymer has a lower ionisation potential than the monomer, the electrochemically obtained polymer is always doped. The oxidative electropolymerisation requires stoichiometric values of 2.07-2.7 Faradays/mol.⁴² The oxidation of the monomer consumes 2 electrons and the excess of charge is due to the doping process. The polymer can be dedoped by repetitive scanning over the neutral range.

The success of electropolymerisation depends highly on the conditions used during the process. The nature of substituents on the monomer (electron-donors or electron-

acceptors), solvents, concentration of the monomer, temperature, nature of the electrodes and electrical conditions are parameters that must be controlled. For example, the presence of water in the solvent can lead to the formation of carbonyl groups along the backbone of the polymer. Another key factor is the nature of the electrolyte. When the polymer is oxidised, the counter anion is bound to the polymer chain to maintain the charge neutrality. The effect of the counter anion can modify the behaviour of the polymer.⁴³

1.5. ORGANIC SOLAR CELLS

The photovoltaic effect is the basic physical process through which a photovoltaic cell converts sunlight into electricity. This effect was discovered by A. E. Becquerel in 1839 and consists of the generation of electricity when photons of a determined wavelength are absorbed by some materials.

In 1954, the first modern solar cell, which presented 5% efficiency, was prepared by Chapin *et al.*⁴⁴ Undoubtedly since then, inorganic materials have been widely used to fabricate solar cells. Although crystalline silicon is the most widely used material, other materials such as amorphous silicon, multicrystalline silicon, III-V compounds (GaAs, InP, GaSb) and chalcogenide copper indium gallium diselenide (CIGS) have been used.⁴⁵ All these compounds present band gaps within the range of 1.1-1.7 eV. To date, the majority of commercialised solar cells use silicon wafer as the light absorber and a *p-n* junction for charge separation.

The discovery and development of organic semiconducting materials led to the preparation of the first organic photovoltaic cell (OPV) in 1985.⁴⁶ This two-layer OPV was prepared by depositing two thin layers of copper phthalocyanine (CuPc) onto indium tin oxide (ITO) and a perylene tetracarboxylic derivative (PV) that was connected to a silver electrode. The device presented a power efficiency of 0.95%.

Nowadays, OPVs can be classified into three different groups (*i*) polymer and small molecules solar cells,⁴⁷ (*ii*) dye-sensitized solar cells,⁴⁸ and (*iii*) hybrid solar cells

based on an organic material acting as a donor and hole transporter and an inorganic material that acts as acceptor and transports electrons.⁴⁷

1.5.1. Solar Energy

Sunlight is Earth's primary source of energy and it has been estimated that around 1000 Wm^{-2} reaches the surface. Although the solar irradiance spreads from 300 up to 4000 nm, most of the intensity is concentrated below 2000 nm (Figure 1.13.). Materials with high band gaps can only absorb a small amount of solar energy, as the photons are not energetic enough to promote electrons from the valence band to the conductance band and generate an electric current. Therefore, low band gap materials are required to maximise the photon harvesting. However, not all the photons with energies larger than the band gap of the materials are absorbed either. The values depicted in Figure 1.13. are only theoretical as the absorption will not be complete and the incident photon to current efficiencies (IPCE) will not reach unity.

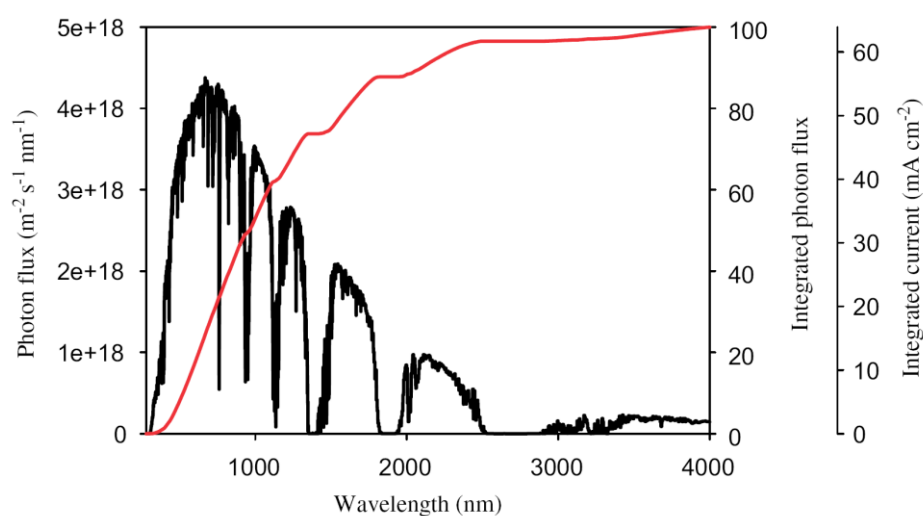


Figure 1.13. Photon flux and integrated current as a function of wavelength.⁴⁹

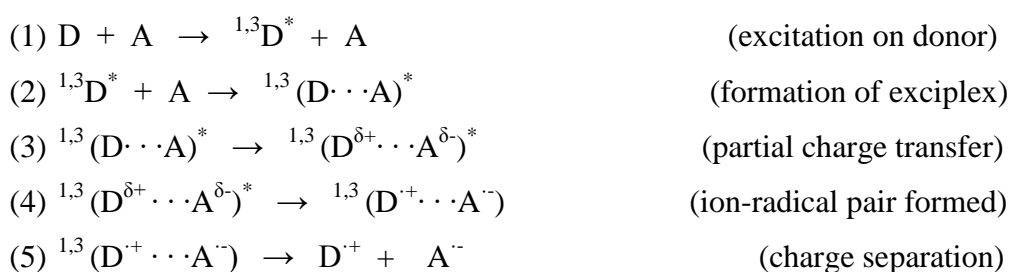
1.5.2. Mechanisms to Turn Light into Electricity

The production of electricity in a solar cell requires the absorption of photons, as described above. When light absorption occurs molecules are excited from the fundamental state S_0 to the excited state S_1 . Singlet-singlet transitions are allowed, and when a photon is absorbed a singlet exciton, with a lifetime of nanoseconds, is formed. The energy gained in the absorption can then decay to the ground state radiatively and this represents luminescence and, in the case of OPV cells, represents a loss mechanism. The exciton energy can also decay to the ground state by vibrations. Another way of decay is *via* intersystem crossing (ISC) that leads to a lower-energy triplet state T_1 . The energy in these states is carried by triplet excitons and the lifetime of these latter species is increased up to microseconds (decay to the ground state is forbidden). If no trapping occurs, triplet excitons can diffuse up to 100 nm. The important feature in solar cells is the fact that the singlet and triplet excitons can decay into geminate pairs of charges leading to charge generation.⁵⁰

Ideally, once the exciton has been formed in the donor (polymer), it diffuses towards a dissociation site within the exciton lifetime before it relaxes to the ground state (*exciton diffusion*). Due to the low exciton diffusion lengths found in polymers (10-20 nm),⁵¹ an appropriate device structure is required to maximise the number of excitons reaching the interphase.

The movement of excitons to the donor/acceptor interface does not imply the existence of free charge carriers (electrons and holes). The charge generation requires large electric fields to compete with coulombic interactions. Both the donor polymer and the acceptor (mainly fullerene) have low dielectric constants that implies that the exciton is coulombically bound at the interface. At the interface strong local electric fields enable the charge separation. At this point the main loss mechanisms occur in the solar cells. The bound exciton cannot split and *geminate recombination* occurs. Bimolecular recombination of free charges can also occur when they are travelling to the electrodes.

Charge separation can occur when the excitons reach the donor/acceptor interphase. In 1992, Heeger *et al.* found that a photoinduced ultrafast charge transfer process occurs between a conjugated polymer and C₆₀.⁵² This was a breakthrough as the vast majority of active layers in OPVs are now based on polymers (donors) and derivatives of C₆₀ (acceptors). The charge transfer process occurs only when $I_{D^*} - A_A - U_C < 0$, where I_{D^*} is the ionization potential of the excited donor, A_A is the electron affinity of the acceptor and U_C is the coulombic energy of the separated radicals. The loss in energy is dissipated by emitting phonons. Therefore, charge generation occurs when the exciton splits with electrons going into the acceptor and holes created in the donor.



The free charge carriers have to travel through the material (*charge transport*), the holes in the donor and the electrons in the acceptor, to reach the electrodes and generate an electric current. The charge mobility in organic semiconductors, which is electric field dependent, is generally low and different factors have to be considered to increase these values. Packing order plays a fundamental role. As an example, the regiorandom polymer poly(3-alkyl-thiophene) presents much lower charge mobility than its regioregular analogue.⁵³

The free charges are then collected at the electrodes (*charge collection*). The holes arrive to a high workfunction electrode, typically ITO, and the electrons are collected at a lower workfunction electrode, typically aluminium.

1.5.3. Device Architectures

The two main structures used in OPVs are a donor-acceptor *bilayer heterojunction* structure and the so-called *bulk heterojunction* (BHJ) structure. The bilayer heterojunction shows an efficient charge generation at the donor-acceptor interface due to their different affinities. In devices prepared with this structure, the bilayer heterojunction of organic materials is sandwiched between the high workfunction electrode, which is similar to the HOMO level of the donor, and the low workfunction electrode which is similar to the LUMO level of the acceptor. Bilayer heterojunctions have been typically fabricated by spin-coating of a donor polymer and evaporated C₆₀ or by sequential evaporation. The main drawback of this type of architecture is that due to the short diffusion lengths of the excitons, only the photons absorbed within 10-20 nm from the heterojunction can be transferred to the acceptor.

In 1995, Yu and co-workers developed a new type of structure, the so-called *bulk heterojunction* (BHJ) (Figure 1.14.).⁵⁴ The BHJ structure is an interpenetrating blend of donor and acceptor components in a bulk volume. In this structure, the distance between donor-acceptor interfaces is shorter than the *exciton diffusion length* overcoming the main drawback of the devices based on bilayer heterojunction. Unlike bilayer heterojunction structures, the intrinsic network in BHJs is intermixed and therefore the charges need percolated pathways to arrive at the electrodes; the workfunction difference is the driving force for this charge percolation. The BHJ solar cells based on poly(3-hexylthiophene) and [6,6]-phenyl-C61-butyric acid methyl ester (PCBM) have been studied thoroughly to understand the key parameters of the structure and efficiencies of around 5% have been obtained.⁵⁵ Nowadays, the vast majority of the high-performance OPVs are fabricated with a BHJ-active layer structure.

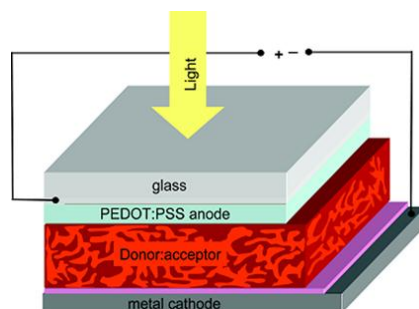


Figure 1.14. Schematic of a BHJ type solar cell.

The working electrodes play a key role in the performance of the OPVs. Aluminium or calcium are usually used as the cathode as their workfunction is similar to the LUMO level of PCBM. In order to have a better contact, usually a layer of LiF is placed between the active layer and the metal. On the other hand, ITO is usually used as the anode as it is a transparent electrode and its workfunction is similar to the HOMO level of the donors. ITO is usually treated with PEDOT:PSS in order to improve the surface quality and to facilitate the hole injection/extraction from the active layer. Additionally, it has been seen that the addition of additives to the active layer (*e.g.*, diiodooctane,) can improve the nanomorphology of the active layer and improve considerably the power conversion efficiency.

1.5.4. Physics of Organic Solar Cells

In order to compare the photovoltaic properties of the fabricated solar cells under irradiation, the illumination conditions are standardised. The Standard Test Conditions for solar cells is the Air Mass 1.5 spectrum, an incident power density of 1000 Wm^{-2} and a temperature of 25°C .⁵⁶ The characteristics of OPVs can be described by the definition of some parameters.

At open circuit conditions V_{OC} (under illumination), the resulting current becomes zero. In OPVs, V_{OC} is related to the difference between the HOMO of the donor and the LUMO of the acceptor (see next section). The nanomorphology of the active layer and charge carrier losses lower the V_{OC} .^{56,57}

Short circuit current (I_{SC}) depends on the photon absorption of the active layer. An ideal circuit (loss free contacts), is determined by the photoinduced charge carrier density and the charge carrier mobility:

$$I_{SC} = ne\mu E \quad (1)$$

where n is the density of charge carriers, e is the elementary charge, μ is the charge mobility and E is the electric field.

The OPV cannot work at these limit conditions and the maximum current (I_{max}) and voltage (V_{max}) are obtained from the maximum power ($P_{max} = I_{max} V_{max}$) the device can deliver.⁵⁶ The fill factor (FF) depends on the charge transport and the recombination process occurring in the solar cell and is defined as:

$$FF = \frac{P_{max}}{I_{sc} V_{oc}} = \frac{I_{max} V_{max}}{I_{sc} V_{oc}} \quad (2)$$

The external quantum efficiency (EQE) or incident photon-to-current efficiency (IPCE) relates the measured photocurrent at short circuit conditions with the number of incident photons.⁵⁶

$$IPCE = \frac{1240 I_{sc}}{\lambda P_{in}} \quad (3)$$

where λ is the incident photon wavelength and P_{in} is the incident power.

Finally the photovoltaic power conversion efficiency (η) of a solar cell is given by:

$$\eta = \frac{V_{oc} I_{sc} FF}{P_{in}} \quad (4)$$

From this equation, it can be deduced that in order to increase the power conversion efficiency of an OPV the product of the numerator has to be maximised. Therefore, not only high I_{SC} and V_{OC} are desired but also high values of FF. The increase of each parameter is a multifactorial combination of design of the active materials (HOMO-LUMO levels, band gap, absorption coefficient, solubility and charge

mobilities) and the fabrication of the device (electrodes, solvent, annealing, nanomorphology, thickness of each component and additives).

1.5.5. Optimum Alignment of the Orbital Levels

For efficient OPVs, a low band gap polymer is not the only requirement. In fact, very low band gaps can be detrimental for the efficiency. In addition to the control of the band gap, the relative HOMO and LUMO energy levels of the donors have to be considered. Assuming a high *fill factor* (FF ~ 0.65), open circuit voltages of approx. $V_{OC} = 0.60-1$ V are needed in OPVs in order to achieve high efficiencies.

As it can be deduced from equation 4, an increase in the value of V_{OC} leads to an increase in the efficiency of the OPV device. In 2006, Scharber *et al.*⁵⁸ demonstrated that the V_{OC} of BHJ devices (using PCBM as an acceptor), and therefore the efficiency, is determined by the HOMO level of the donor and the LUMO level of the acceptor molecule, such that:

$$V_{OC} = (1/e) (| E^{Donor} HOMO | - | E^{PCBM} LUMO |) - 0.3 \text{ V} \quad (5)$$

where e is the elementary charge and the value of 0.3 V is an empirical factor.

Derived from those findings, a relationship between the efficiency of a BHJ solar cell, band gap and the LUMO level of the donor was derived (Figure 1.15.).

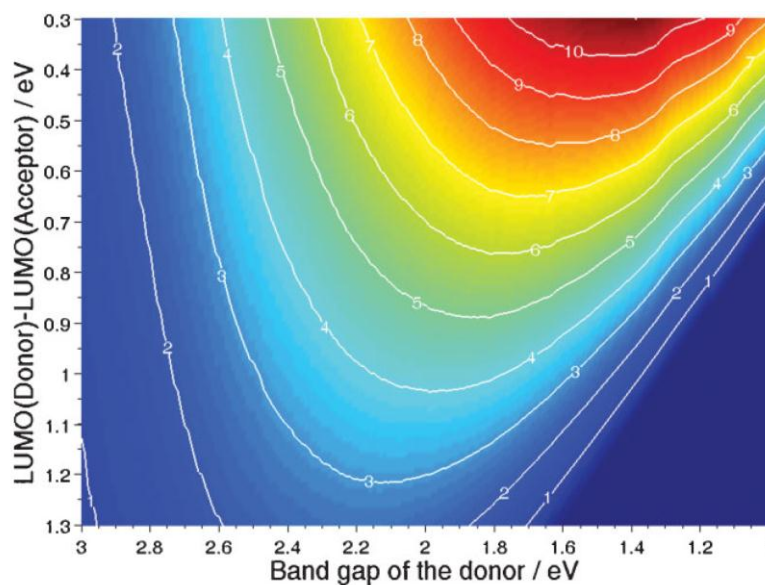


Figure 1.15. Contour plot showing the calculated energy-conversion efficiency (contour lines and colours) versus the band gap and the LUMO level of the donor polymer.⁵⁸

For an efficient charge generation, an appropriate LUMO-LUMO donor-acceptor offset is required. The energy offset between both LUMO levels facilitates charge separation. A large difference between the LUMO values leads to loss of energy as the electron in the donor LUMO is transferred to a lower energy level than the acceptor LUMO.⁵⁹ It has been demonstrated that values within 0.3-0.5 eV are required to achieve charge separation. The difference between the LUMO of the donor and acceptor are usually higher than this value. Therefore, in order to decrease the offset and increase the device efficiency, three approaches can be followed:

- i) Reducing the LUMO level of the donor. As long as the HOMO level does not change, a polymer with a lower band gap is obtained and the V_{OC} remains constant.
- ii) The second approach is to reduce both the HOMO and the LUMO levels. In this case the band gap remains constant, but the offset has been lowered and the V_{OC} is increased.
- iii) The last approach to diminish the offset is to increase the LUMO level of the acceptor.

1.5.6. Materials

Poly(3-hexyl-thiophene) has been widely used, in combination with PCBM in BHJ solar cells.⁵⁵ However, the relatively high band gap of P3HT and the poor match of its absorption spectrum with the solar illumination profile limits the efficiencies of these devices.²⁰ In general, the efficiencies of homopolymers are low as they usually show large band gaps (> 1.9 eV). In order to obtain low band gap polymers and a higher absorption match, different organic moieties and design strategies have been developed. The aforementioned approaches to decrease the band gaps of the conjugated systems have been followed (stabilisation of the quinoid form and donor-acceptor approaches).

The most commonly used donor (electron-rich) molecules are based on thiophene and benzene rings units. Due to the higher aromaticity and electron-deficiency of the latter, the co-monomers generally show deeper HOMO levels. The desired planarity of the polymers can be achieved by the bridging of adjacent units to give multiple fused-rings (see Figure 1.16.). These moieties can be seen as two rings (thiophene or benzene) linked by C, N, Si or Ge atoms.⁶⁰

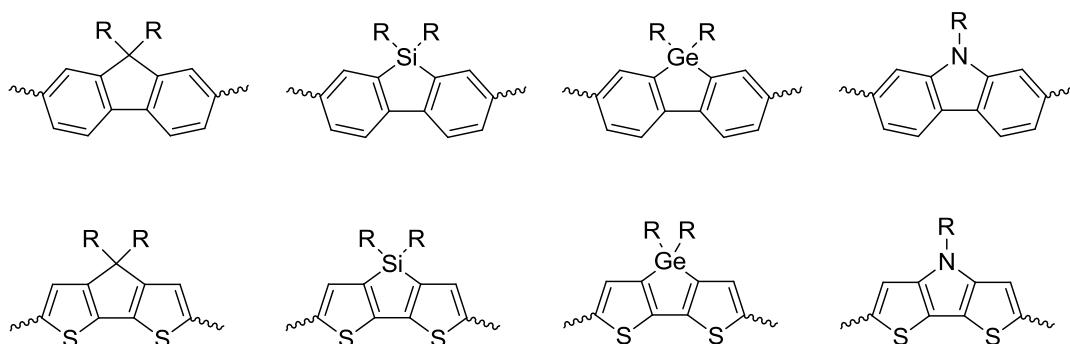


Figure 1.16. Chemical structure of some donor units.

On the other hand, the most utilised acceptor (electron-poor) units include an imine (C=N) or carbonyl (C=O) group attached to thiophene or benzene rings to increase the electron affinity. The importance of synthesising low LUMO lying polymers

relies on the fact that as deep HOMO levels are required, to achieve low band gaps, the LUMO has to be decreased. Typical acceptor units are shown in Figure 1.18.⁶⁰



Figure 1.17. Chemical structure of some acceptor units.

Whereas most of the synthesis has been focused on the development of donor materials, the investigation of different acceptors has not attracted so much interest. The vast majority of OPVs have been fabricated using fullerene derivatives such as C_{60} . In 1995, Wudl *et al* prepared $PC_{61}BM$ (**9**), which, due to its solubility, has been widely used in OPVs.⁶¹ These materials show high electron-affinities with low lying LUMO levels (~ 4.2 eV for $PC_{61}BM$) and high electron mobilities. In the past few years, $PC_{71}BM$ has been used in high efficiency OPVs as its lower symmetry compared to $PC_{61}BM$ increases the absorption range (300-600 nm).⁶² Apart from fullerene derivatives, other compounds have been also studied as acceptors, but only rylene diimide derivatives have shown efficiencies over 2%.⁶³

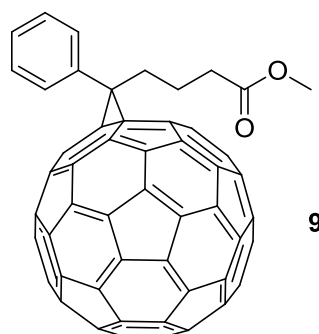


Figure 1.18. Chemical structure of $PC_{61}BM$.

1.6. ORGANIC FIELD EFFECT TRANSISTORS (OFETs)

Transistors are on/off switches in electronic circuits that are controlled by an applied voltage. Since 1986, when the first organic field-effect transistor (OFET) was reported comprising of polythiophene as the organic semiconductor with a charge carrier mobility of $10^{-5} \text{ cm}^2 \cdot \text{V}^{-1} \cdot \text{s}^{-1}$, OFETs have been widely studied.⁶⁴

Generally, OFETs are fabricated with three electrodes (gate, source and drain), an insulating dielectric material and a semiconducting organic material. Usually doped silicon acts as gate the electrode and an insulating material (SiO_2). Other dielectrics have also been used (inorganic materials, insulator polymers) as gate dielectrics.⁶⁵ For *p*-type organic materials, metals with a high work-function ($\Phi(\text{platinum}) = -6.35 \text{ eV}$ and $\Phi(\text{gold}) = -5.1 \text{ eV}$) are needed in order to obtain ohmic contact with the HOMO level of the semiconductor. On the other hand, low work-function metals ($\Phi(\text{calcium}) = -2.87 \text{ eV}$; $\Phi(\text{lithium}) = -2.93 \text{ eV}$ and $\Phi(\text{aluminum}) = 2.87 \text{ eV}$) are used as electrodes for *n*-type materials.⁶⁶

OFETs have been prepared from single molecules, oligomers or polymers. The vast majority of them act as *p*-type materials (hole-conductors). *n*-Type semiconductors are less common and they are compounds with a high electron-affinity. Hole and electron mobility in a device can be achieved by incorporating a *p*-type and an *n*-type semiconductor in the device. A bilayer and a blend of both materials are approaches that were used previously. Recently, ambipolar semiconductors with high mobilities have been synthesised and single-component OFETs have been fabricated.⁶⁵

The main structures of OFETs are depicted in Figure 1.19. Typically the structures are classified as bottom-gate and top-gate devices.⁶⁷ In the first case (bottom contact-bottom gate), the semiconducting layer is deposited on the substrate where the electrodes (source and drain) have been incorporated. In top contact-bottom gate OFETs, the semiconductor is placed on the insulator and the electrodes are evaporated through a shadow mask. In the third structure, both the insulating layer and the gate electrode are placed over the semiconducting material.

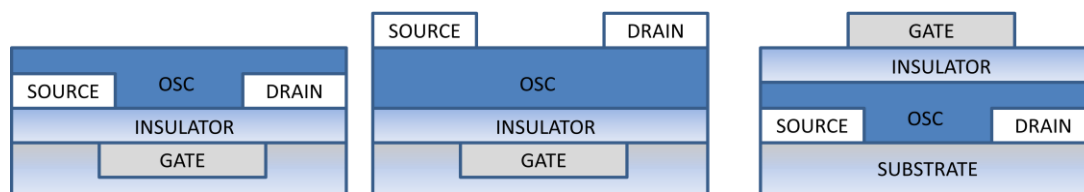


Figure 1.19. Typical OFET architectures: a) bottom contact-bottom gate, b) top contact-bottom gate and c) bottom contact-top gate.

The operation of OFETs is based on the application of a voltage at the gate electrode (V_g) that induces a large electric field between the insulator and the organic semiconductor. If no voltage is applied between the source and drain electrodes, the semiconductor should not conduct the electricity and the current should be zero. On the other hand, when a voltage is applied between the source and the drain (V_{ds}), charge-carriers are injected and the current can be produced. The source is the charge injector and when the gate voltage is negative ($V_g < 0$), the source voltage (V_s , which is normally grounded and therefore 0 V) is always more positive than V_g and holes are injected to the HOMO (p -channel). When the gate voltage is positive ($V_g > 0$), V_s is more negative and electrons are injected in the LUMO (n -channel) from the source.^{65,67}

The performance of OFET operation is mainly governed by three parameters. Threshold voltage (V_{th}) arises from the presence of charge traps that have to be filled and therefore the effective gate voltage is ($V_g - V_{th}$). If $V_g < V_{th}$, there is no injection of charge carries into semiconductor. The ratio I_{on}/I_{off} relates the drain current at a particular gate voltage (on-state) and the drain gate current in the off-state ($V_g = 0$). High I_{on}/I_{off} ratios are desired for efficient switching behaviour in transistors. Obviously, I_{off} should be low. Doping impurities in the organic semiconductor layer can lead to undesired I_{off} . The mobility of the charges (μ_e and μ_h) is a key factor for the high performance of an OFET. The field-effect mobility of the charge carriers depends on the extent of π -overlap in the molecular structure and the molecular ordering. Charge-mobilities higher than $0.1 \text{ cm}^2\text{V}^{-1}\text{s}^{-1}$ are required for high-speed electronic circuits.^{67,65,68}

The I-V characteristics of the OFETs can be studied from the above measurements. The drain current (I_d) can be measured at constant V_{ds} and different V_g or by varying the V_{ds} and maintaining the V_g constant. I_d can be expressed as:⁶⁵

$$I_d = \frac{W}{L} \mu C_i \left[(V_g - V_{Th}) V_{ds} - \frac{1}{2} V_{ds}^2 \right] \quad (6)$$

where W is channel width, L is the length between source-gate electrodes, μ is the field-effect mobility and C_i is the capacitance of the insulator. Depending on the gate voltage, the drain current input shows two regimes. When V_{ds} is low ($V_{ds} \ll V_g$), the behaviour of the current is linearly proportional to the V_g and equation 7 can be reduced to:

$$I_d = \frac{W}{L} \mu_{lin} C_i (V_g - V_{Th}) V_{ds} \quad (7)$$

where the field-effect mobility is assumed to be gate voltage independent.^{65,68}

When $V_{ds} = V_g - V_{Th}$, the current I_d does not increase substantially and regime of saturation is reached where Equation 6 can be written as:

$$I_{d,sat} = \frac{W}{2L} \mu_{sat} C_i (V_g - V_{Th})^2 \quad (8)$$

A typical graph (output characteristics) where V_{ds} versus I_d is plotted is shown in Figure 1.20.^{65,68} This figure shows the behaviour of the I_d when V_{ds} is varied at different V_g . From the slope of the curves in the linear regime, μ_{lin} can be calculated. μ_{sat} can be calculated by plotting $\sqrt{|I_d|}$ versus V_g . These values might be different as result of the of different electric-field distributions.⁶⁹

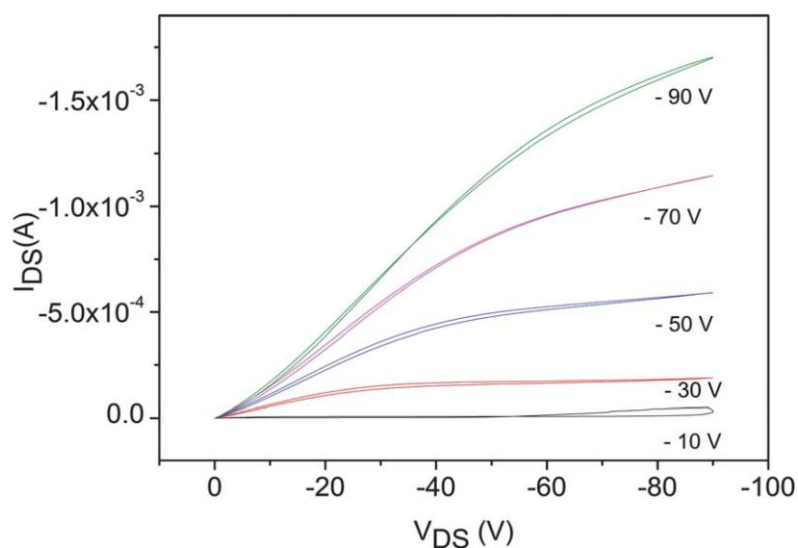


Figure 1.20. Typical output characteristics of OFETs.

1.7. ORGANIC LIGHT EMITTING DIODES (OLEDs)

In 1990, researchers from the Cavendish Laboratory in Cambridge applied a voltage to a conducting plastic film of PPV and observed that it emitted a greenish light.⁷⁰ This was the first step towards organic light-emitting diodes OLEDs.

Since then, OLEDs have been mainly prepared using small organic molecules, oligomers and polymers. OLEDs using polymers as the organic compound are so-called polymer light-emitting diodes PLEDs. In these diodes, an electrical current is applied to the device in which an electroluminescent conductive polymer emits light. Basically, it can be said that OLEDs work in a similar, but opposite way to photovoltaic devices where the electromagnetic energy coming from the sun is converted into electrical energy.⁷¹

A simple OLED can be prepared by depositing a conducting electroluminescent organic material between two thin-film electrodes. Usually, indium tin oxide (ITO) is used as the anode, which is transparent to visible light, and calcium is used as the

cathode, although this metal can give stability problems. A schematic picture of an OLED is shown below in Figure 1.21.⁷¹

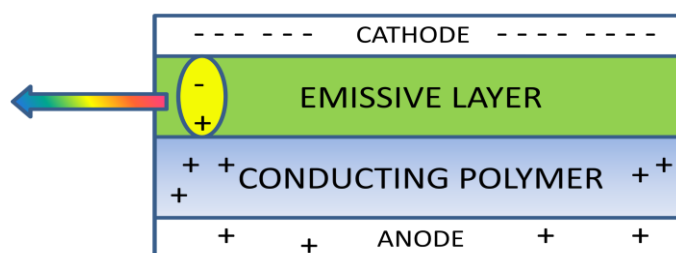


Figure 1.21. Schematic of a simple OLED

When a voltage is applied to the electrodes, an electric current flows through the device from the cathode to the anode. During this process, electrons and holes are injected into the semiconductor layer. The recombination of electrons and holes leads to the formation of singlet excitons that decay radiatively and results in the emission of visible light. The performance of OLEDs is critically dependent on the efficient injection of electrons from the cathode of low work function into the organic semiconductor.⁷¹

More developed OLEDs show more complicated structures. Two organic layers can be sandwiched between the electrodes. The first one is a *conductive layer* placed between the anode and the second layer, the so-called *emissive layer*, is sandwiched between the former layer and the cathode. In this kind of OLED, the holes coming from the conductive layer are transported into the emissive layer and recombine with the electrons emitting light. Even more complicated OLEDs show multilayer structures that can have more than two layers to improve the device efficiency.⁷¹

1.8. ELECTROCHROMISM

Since its discovery in 1966,⁷² different types of electrochromic materials have been developed. Mainly they are metal oxide films, molecular dyes and conducting

polymers. These materials have the capacity to change reversibly their optical properties, *i.e.* colour, when a voltage is applied. When a voltage is applied, the electrochromic material undergoes a process of oxidation or reduction. These redox reactions lead to a change in the electronic levels. Therefore, the absorption wavelength of the doped material is modified and a colour change can be observed.

The key properties of electrochromic devices (ECDs) are rapid switching times (determined by colouring time t_c and bleaching time t_b), high contrast ratios ($\Delta\%T$ where T is transmittance), colouration efficiency, electrochromic memory and long-term stability.

A typical ECD is formed by seven different layers (Figure 1.22). The active part of the ECD, which is formed by the electrochromic material, electrolyte and ion storage layers, is sandwiched between two transparent substrates and electrodes. These devices have been used in displays, smart windows and mirrors and active optical filters.⁷³

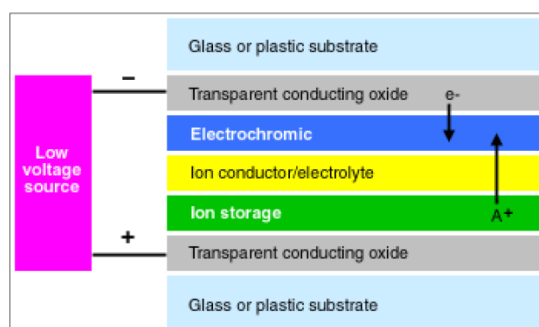


Figure 1.22. Typical structure of an electrochromic device (ECD).

Conjugated polymers, such as polypyrrole, polyaniline, polythiophene and their derivatives, have been widely used for electrochromic applications.⁷⁴ One of the main advantages of these polymers is that it is relatively easy to modify their colouration by attaching different substituents to the main conjugated chain. By following this approach, a wide number of different colours can be obtained.

REFERENCES

1. H. N. McCoy and W. C. Moore, *Journal of the American Chemical Society*, 1911, **33**, 273.
2. H. Akamatu, H. Inokuchi and Y. Matsunaga, *Nature*, 1954, **173**, 168.
3. R. G. Kepler, P. E. Bierstedt and R. E. Merrifield, *Physical Review Letters*, 1960, **5**, 503.
4. F. Wudl, G. M. Smith and E. J. Hufnagel, *J. Chem. Soc., Chem. Comm.*, 1970, 1453.
5. J. Ferraris, D. O. Cowan, V. Walatka and J. H. Perlstein, *Journal of the American Chemical Society*, 1973, **95**, 948.
6. K. Bechgaard, C. S. Jacobsen, K. Mortensen, H. J. Pedersen and N. Thorup, *Solid State Communications*, 1980, **33**, 1119.
7. H. Tatemitsu, E. Nishikawa, Y. Sakata and S. Misumi, *Journal of the Chemical Society, Chemical Communications*, 1985, 106.
8. A. F. Hebard, M. J. Rosseinsky, R. C. Haddon, D. W. Murphy, S. H. Glarum, T. T. M. Palstra, A. P. Ramirez and A. R. Kortan, *Nature*, 1991, **350**, 600.
9. O. ZHOU, Q. ZHU, J. E. FISCHER, N. COUSTEL, G. B. M. VAUGHAN, P. A. HEINEY, J. P. MCCAULEY and A. B. SMITH, *Science*, 1992, **255**, 833.
10. G. Saito and Y. Yoshida, *The Chemical Record*, 2011, **11**, 124.
11. B. Bolto, R. McNeill and D. Weiss, *Australian Journal of Chemistry*, 1963, **16**, 1090.
12. J. McGinness, P. Corry and P. Proctor, *Science*, 1974, **183**, 853.
13. H. Shirakawa, E. J. Louis, A. G. MacDiarmid, C. K. Chiang and A. J. Heeger, *Journal of the Chemical Society, Chemical Communications*, 1977, 578.
14. C. K. Chiang, M. A. Druy, S. C. Gau, A. J. Heeger, E. J. Louis, A. G. MacDiarmid, Y. W. Park and H. Shirakawa, *Journal of the American Chemical Society*, 1978, **100**, 1013.
15. T. A. Skotheim and J. Reynolds, *Handbook of Conducting Polymers*, 3 edition edn., CRC Press, 2007.

16. *Handbook of Organic Conductive Molecules and Polymers*, John Wiley & Sons, 1997.
17. K. J. Laidler and J. H. Meiser, *Physical Chemistry*, Third sub edition edn., Houghton Mifflin Company, 1999.
18. P. Atkins and J. d. Paula, *Atkins' Physical Chemistry*, senenth edition edn., Oxford University Press Inc., New York, 2002.
19. S. Elliott, *The Physics and Chemistry of Solids*, Wiley-Blackwell, 1998.
20. J. Roncali, *Chemical Reviews*, 1997, **97**, 173.
21. T. Izumi, S. Kobashi, K. Takimiya, Y. Aso and T. Otsubo, *Journal of the American Chemical Society*, 2003, **125**, 5286.
22. J. L. Bredas, *The Journal of Chemical Physics*, 1985, **82**, 3808.
23. F. Wudl, M. Kobayashi and A. J. Heeger, *The Journal of Organic Chemistry*, 1984, **49**, 3382.
24. J. Roncali, *Macromolecular Rapid Communications*, 2007, **28**, 1761.
25. E. E. Havinga, W. Hoeve and H. Wynberg, *Polymer Bulletin*, 1992, **29**, 119.
26. P. Berrouard, A. Najari, A. Pron, D. Gendron, P.-O. Morin, J.-R. Pouliot, J. Veilleux and M. Leclerc, *Angewandte Chemie International Edition*, 2012, **51**, 2068.
27. A. Facchetti, L. Vaccaro and A. Marrocchi, *Angewandte Chemie International Edition*, 2012, **51**, 3520.
28. J. K. Stille, *Angewandte Chemie International Edition in English*, 1986, **25**, 508.
29. Z. Bao, W. Chan and L. Yu, *Chemistry of Materials*, 1993, **5**, 2.
30. B. Carsten, F. He, H. J. Son, T. Xu and L. Yu, *Chemical Reviews*, 2011, **111**, 1493.
31. N. Miyaura and A. Suzuki, *Chemical Reviews*, 1995, **95**, 2457.
32. T. E. Barder, S. D. Walker, J. R. Martinelli and S. L. Buchwald, *Journal of the American Chemical Society*, 2005, **127**, 4685.
33. T. Yamamoto, T. Maruyama, Z. H. Zhou, Y. Miyazaki, T. Kanbara and K. Sanechika, *Synthetic Metals*, 1991, **41**, 345.

34. T. Yamamoto, A. Morita, Y. Miyazaki, T. Maruyama, H. Wakayama, Z. H. Zhou, Y. Nakamura, T. Kanbara, S. Sasaki and K. Kubota, *Macromolecules*, 1992, **25**, 1214.
35. T. Yamamoto, T. Maruyama, Z.-H. Zhou, T. Ito, T. Fukuda, Y. Yoneda, F. Begum, T. Ikeda and S. Sasaki, *Journal of the American Chemical Society*, 1994, **116**, 4832.
36. R. D. McCullough, *Advanced Materials*, 1998, **10**, 93.
37. K. Yoshino, S. Hayashi and R.-i. Sugimoto, *Japanese Journal of Applied Physics*, 1984, **23**, L899.
38. M. Pomerantz, J. J. Tseng, H. Zhu, S. J. Sproull, J. R. Reynolds, R. Uitz, H. J. Arnott and M. I. Haider, *Synthetic Metals*, 1991, **41**, 825.
39. M. R. Andersson, D. Selse, M. Berggren, H. Jaervinen, T. Hjertberg, O. Inganaes, O. Wennerstroem and J. E. Oesterholm, *Macromolecules*, 1994, **27**, 6503.
40. V. M. Niemi, P. Knuutila, J. E. Österholm and J. Korvola, *Polymer*, 1992, **33**, 1559.
41. *Handbook of Thiophene-Based Materials*, John Wiley & Sons Ltd., 2009.
42. J. Roncali, *Chemical Reviews*, 1992, **92**, 711.
43. W. Domagala, D. Palutkiewicz, D. Cortizo-Lacalle, A. L. Kanibolotsky and P. J. Skabara, *Optical Materials*, 2011, **33**, 1405.
44. D. M. Chapin, C. S. Fuller and G. L. Pearson, *J. Appl. Phys.* , 1954, **25**, 676.
45. L. El Chaar, L. A. lamont and N. El Zein, *Renewable and Sustainable Energy Reviews*, 2011, **15**, 2165.
46. C. W. Tang, *Applied Physics Letters*, 1986, **48**, 183.
47. F. G. Brunetti, R. Kumar and F. Wudl, *Journal of Materials Chemistry*, 2010, **20**, 2934.
48. B. O'Regan and M. Gratzel, *Nature*, 1991, **353**, 737.
49. R. Kroon, M. Lenes, J. C. Hummelen, P. W. M. Blom and B. de Boer, *Polymer Reviews*, 2008, **48**, 531.
50. J.-M. Nunzi, *Comptes Rendus Physique*, 2002, **3**, 523.

51. A. Haugeneder, M. Neges, C. Kallinger, W. Spirkl, U. Lemmer, J. Feldmann, U. Scherf, E. Harth, A. Gügel and K. Müllen, *Physical Review B*, 1999, **59**, 15346.
52. N. S. Sariciftci, L. Smilowitz, A. J. Heeger and F. Wudl, *Science*, 1992, **258**, 1474.
53. G. Juska, K. Arlauskas, R. Österbacka and H. Stubb, *Synthetic Metals*, 2000, **109**, 173.
54. G. Yu, J. Gao, J. C. Hummelen, F. Wudl and A. J. Heeger, *Science*, 1995, **270**, 1789.
55. W. Ma, C. Yang, X. Gong, K. Lee and A. J. Heeger, *Advanced Functional Materials*, 2005, **15**, 1617.
56. S. Günes, H. Neugebauer and N. S. Sariciftci, *Chemical Reviews*, 2007, **107**, 1324.
57. A. Moliton and J.-M. Nunzi, *Polymer International*, 2006, **55**, 583.
58. M. C. Scharber, D. Mühlbacher, M. Koppe, P. Denk, C. Waldauf, A. J. Heeger and C. J. Brabec, *Advanced Materials*, 2006, **18**, 789.
59. J. J. M. Halls, J. Cornil, D. A. dos Santos, R. Silbey, D. H. Hwang, A. B. Holmes, J. L. Brédas and R. H. Friend, *Physical Review B*, 1999, **60**, 5721.
60. C. Duan, F. Huang and Y. Cao, *Journal of Materials Chemistry*, 2012, **22**, 10416.
61. J. C. Hummelen, B. W. Knight, F. LePeq, F. Wudl, J. Yao and C. L. Wilkins, *The Journal of Organic Chemistry*, 1995, **60**, 532.
62. C.-Z. Li, H.-L. Yip and A. K. Y. Jen, *Journal of Materials Chemistry*, 2012, **22**, 4161.
63. P. Sonar, J. P. Fong Lim and K. L. Chan, *Energy & Environmental Science*, 2011, **4**, 1558.
64. A. Tsumura, H. Koezuka and T. Ando, *Applied Physics Letters*, 1986, **49**, 1210.
65. J. Zaumseil and H. Sirringhaus, *Chemical Reviews*, 2007, **107**, 1296.
66. A. R. Murphy and J. M. J. Fréchet, *Chemical Reviews*, 2007, **107**, 1066.
67. G. Horowitz, *Advanced Materials*, 1998, **10**, 365.

68. C. D. Dimitrakopoulos and P. R. L. Malenfant, *Advanced Materials*, 2002, **14**, 99.
69. V. Coropceanu, J. Cornil, D. A. da Silva Filho, Y. Olivier, R. Silbey and J.-L. Brédas, *Chemical Reviews*, 2007, **107**, 926.
70. J. H. Burroughes, D. D. C. Bradley, A. R. Brown, R. N. Marks, K. Mackay, R. H. Friend, P. L. Burns and A. B. Holmes, *Nature*, 1990, **347**, 539.
71. A. C. Grimsdale, K. Leok Chan, R. E. Martin, P. G. Jokisz and A. B. Holmes, *Chemical Reviews*, 2009, **109**, 897.
72. S. K. Deb and J. A. Chopoorian, *Journal of Applied Physics*, 1966, **37**, 4818.
73. P. M. S. Monk, R. J. Mortimer and D. R. Rosseinsky, *Electrochromism and Electrochromic Devices*, Cambridge University Press, Cambridge, UK, 2007.
74. P. M. Beaujuge and J. R. Reynolds, *Chemical Reviews*, 2010, **110**, 268.